Mol Gen Genomics (2005) 274: 103–118
DOI 10.1007/s00438-005-0010-y

ORIGINAL PAPER

Kerstin Kaufmann · Nicole Anfang · Heinz Saedler
Günter Theissen

Mutant analysis, protein–protein interactions and subcellular localization of the Arabidopsis B_{sister} (ABS) protein

Received: 23 December 2004 / Accepted: 10 May 2005 / Published online: 4 August 2005

Abstract Recently, close relatives of class B floral homeotic genes, termed B_{sister} genes, have been identified in both angiosperms and gymnosperms. In contrast to the B genes themselves, B_{sister} genes are exclusively expressed in female reproductive organs, especially in the envelopes or integuments surrounding the ovules. This suggests an important ancient function in ovule or seed development for B_{sister} genes, which has been conserved for about 300 million years. However, investigation of the first loss-of-function mutant for a B_{sister} gene (*ABS*/*TT16* from *Arabidopsis*) revealed only a weak phenotype affecting endothelium formation. Here, we present an analysis of two additional mutant alleles, which corroborates this weak phenotype. Transgenic plants that ectopically express *ABS* show changes in the growth and identity of floral organs, suggesting that ABS can interact with floral homeotic proteins. Yeast-two-hybrid and three-hybrid analyses indicated that ABS can form dimers with SEPALLATA (SEP) floral homeotic proteins and multimeric complexes that also include the AGAMOUS-like proteins SEEDSTICK (STK) or SHATTERPROOF1/2 (SHP1, SHP2). These data suggest that the formation of multimeric transcription factor complexes might be a general phenomenon among MIKC-type MADS-domain proteins in angiosperms. Heterodimerization of ABS with SEP3 was confirmed by gel retardation assays. Fusion proteins tagged with CFP (Cyan Fluorescent Protein) and YFP (Yellow Fluorescent Protein) in *Arabidopsis* protoplasts showed that ABS is localized in the nucleus. Phylogenetic analysis revealed the presence of a structurally deviant, but closely related, paralogue of *ABS* in the *Arabidopsis* genome. Thus the evolutionary developmental genetics of B_{sister} genes can probably only be understood as part of a complex and redundant gene network that may govern ovule formation in a conserved manner, which has yet to be fully explored.

Keywords MADS-box proteins · Seed development · B_{sister} · ABS · TT16

Communicated by G. Jürgens

K. Kaufmann · N. Anfang · G. Theissen (✉)
Lehrstuhl für Genetik, Friedrich-Schiller-Universität Jena,
Philosophenweg 12, 07743 Jena, Germany
E-mail: guenter.theissen@uni-jena.de
Tel.: +49-3641-949550
Fax: +49-3641-949552

H. Saedler
Max-Planck-Institut für Züchtungsforschung,
Carl-von-Linné-Weg 10, 50829 Köln, Germany

Present address: N. Anfang
School of Biological Sciences, University of Auckland, Private Bag 92019, Auckland, New Zealand

Introduction

The ovule is the major characteristic feature of seed plants. It comprises a megasporangium, termed the nucellus, which is protected by integuments and allows the megaspore, and later the female gametophyte (embryo sac), to be retained on the mother plant. A number of genes are required for primordium initiation, pattern formation and morphogenesis of ovules (Grossniklaus and Schneitz 1998). In particular, *INNER NO OUTER INO*), *NOZZLE* (*NZZ*, also known as *SPOROCYTELESS*,*SPL*) and *WUSCHEL* (*WUS*) have been identified as key regulators of integument formation. Morphogenesis of the integuments is initiated at an early stage of ovule development and is marked by the transformation of a uniform protrusion into a patterned ovule primordium (Schneitz et al. 1995). Both inner and outer integuments are of epidermal origin. While the outer integument remains bilayered at all stages and shows typical vacuolization, the inner layer of the inner integument differentiates into an endothelium. The endothelium is characterized by compact cells, with little or no vacuolization, which produce proanthocyanidin

(PA). Oxidation of this pigment is responsible for the brown colour of seeds. Seed pigmentation is in turn essential for seed dormancy, longevity and resistance to various external influences (Debeaujon et al. 2003). To date, more than 20 mutants that are defective in seed pigmentation have been isolated, the majority of which are affected in the regulation of PA synthesis. Most of the genes identified so far encode transcription factors that regulate *BANYULS* (*BAN*) expression, which converts leucoanthocyanidins into their corresponding 2,3-*cis*-flavan-3-ols and is the core enzyme of the PA subpathway. A second group of genes is directly involved in endothelium development and includes *TT1*, which encodes a member of the WIP subfamily of zinc-finger transcription factors, and *ABS*/*TT16*/*AGL32* (henceforth termed *ABS*), a MADS-box gene (Becker et al. 2002; Nesi et al. 2002; Sagasser et al. 2002; Becker and Theissen 2003).

ABS has been shown to be involved in seed pigmentation in *Arabidopsis* (Nesi et al. 2002). *abs* mutants have defects in the structure of the inner integument; in particular, they show enhanced vacuolization in the endothelium (Nesi et al. 2002; Debeaujon et al. 2003). *ABS* encodes a MIKC-type MADS-domain protein. Such proteins are characterized by four domains: the MADS-domain, the Intervening region, the K-domain and the C-terminal region (Ma et al. 1991). Most MIKC-type proteins can be assigned by phylogenetic analysis to well-defined subfamilies, which are conserved among seed plants (Becker and Theissen 2003). MIKC-type genes are involved in important aspects of plant reproductive development, such as flower initiation, specification of floral meristem and organ identity, as well as in ovule and fruit development (for a review, see Becker and Theissen 2003). Recently, Pinyopich et al. (2003) have demonstrated that members of the subfamily of *AGAMOUS*-like MIKC-type genes act redundantly in the determination of ovule identity in *Arabidopsis*. The proteins they encode, SEEDSTICK (STK), SHATTERPROOF1 (SHP1) and SHP2, probably function as multimeric complexes together with AGL2-like (SEPALLATA, SEP) proteins (Favaro et al. 2003; Ditta et al. 2004).

ABS belongs to the B_{sister} subfamily of MIKC-type genes, which was only recently identified. Representatives are found both in flowering plants and in gymnosperms (Becker et al. 2002). B_{sister} genes have some intriguing features. In phylogenetic trees, they form a sister group with class B floral homeotic genes, although this grouping is not always well supported (Becker et al. 2002; Carlsbecker et al. 2003; Stellari et al. 2004). However, in strong contrast to B genes, B_{sister} genes are predominantly expressed in female reproductive organs (mainly in ovules) and this expression pattern is conserved among seed plants (Becker et al. 2002). Their evolutionary conservation for at least 300 million years suggests an important function for these genes in ovules; however, the first mutant phenotype described for a B_{sister} gene, the *ABS* gene of *Arabidopsis*, turned out to be relatively weak affecting seed coloration, but not ovule function (Nesi et al. 2002). So in order to gain a better understanding of the developmental function of B_{sister} genes, a more detailed study of the group was initiated in the model plant *Arabidopsis thaliana*.

As a first step towards this goal, we have characterized novel loss- and gain-of-function mutants of *ABS*, determined the subcellular localization of the ABS protein and studied its interaction with other MIKC-type proteins. We have also identified and characterized its most closely related paralogue in the *Arabidopsis* genome. Our results suggest that the evolutionary developmental genetics of B_{sister} genes can only be understood as in the context of a complex and redundant protein interaction network that may govern ovule formation in a conserved manner. This network is yet to be fully explored.

Materials and methods

Plant material and growth conditions

Arabidopsis thaliana (Heyn.) plants, ecotype Columbia-0 (Col-0),were grown in the greenhouse or in phytochambers in plastic trays filled with commercial soil mixture (type ED73; Werkverband) or with a 'home-made' mixture, composed of fertilized peat/vermiculite/sand (8:1:1). For stratification, seeds were kept on the soil for 3–4 days at 4°C in the dark and then cultivated under a 16-h-light/8-h-dark (long-day) photoperiod regime.

Isolation of loss-of-function mutants by reverse genetics

A filter screen on an *En*-mutagenized population of *Arabidopsis* was performed by the ZIGIA Unit (MPIZ Cologne) as described by Steiner-Lange et al. (2001). Seven lines were identified in this screen and the presence of the transposon was confirmed with a PCR-based assay, using the gene-specific primers ABSWiscUni (5′-ATCCAACCTCAATCTCCGTTTCCAGAT-3′) and ABSWiscRev (5′-AGGTAATGGCCAATCTTCACTT CAAAACA-3′), which amplify a genomic fragment of approximately 2.5 kb, and the transposon-specific primers En205 and En8130 (Steiner-Lange et al. 2001). The reaction parameters were as follows: 96°C for 5 min, followed by 36 cycles of 94°C for 15 s, 64°C for 30 s, and 72°C for 2 min, and a final extension step at 72°C for 10 min. PCR products containing putative transposon-flanking sequences were purified using the Qiagen PCR Product Purification kit, and then sequenced.

Southern analysis using a 3′ terminal transposon fragment (En7630, En8164; Steiner-Lange et al. 2001) as a probe was performed as described previously. The identification of excision events (revertant screen) was done using a PCR-based approach with primers that amplify a 200-bp region around the transposon insertion points in the *ABS* locus in the lines 7K66 and 7AAL63.

PCR products were purified and sequenced directly or cloned into pGEM-T (Promega, Madison, WI, USA).

Construction of transgenic 35S::ABS plants

The full-length *ABS* ORF was cloned into pRT100 (Töpfer et al. 1987) via *Apa*I and *Bam*HI restriction sites introduced by PCR using the primers ESTAPAuni (5′-GAAGAAGGGGCCCATGGGTAGAGGG-3′) and ESTBamRev (5′-ATTGAGGATCCTATTAATCATTC TGGG-3′). The construct containing the 35S promoter, the ORF and polyadenylation signal was subcloned into pBAR-A (G. Cardon, unpublished data) via *Eco*RI sites, as described in Winter et al. (2002a). *Arabidopsis* transformation by the *Agrobacterium tumefaciens* strain GV3101/pMP90 (using the floral-dip method) and selection for transgenic T1 plants using Basta was performed as described previously (Winter et al. 2002a). The 35S::*ABS*-MIK transgenic plants were generated in the same way. The MIK deletion construct encodes amino acids 1–173 of the ABS protein. Genomic PCR for amplification of both constructs from transgenic plants was performed using the primers CmV1 (5′-CTTGCATGCCTGCAGGTCAACATGG-3′) and PtM7 (3′-CACTGGATTTGGTTTTAGGAATTAG-5′). Southern analysis of DNA from pooled T2 plants of 35S::*ABS*-MIKC lines was performed using a radioactively labelled 300-bp fragment of the *BAR* gene as a probe, which was amplified using the primers 555 (5′-AC CTGCTGAAGTCCCTGGAGG-3′) and 557 (3′-AAA GAACGTGGACTCCAACGTCAAAG-5′). RT-PCR was performed using gene-specific primers for *ABS*, *SHP1*, *SHP2*, *AG* and *AGL63* coding sequences.

Stereomicroscopic and SEM analysis

A binocular microscope (Leica, Wetzlar, Germany) equipped with a digital camera was used to take pictures of floral buds, flowers and siliques.

Scanning electron microscopy was performed as described by Unte et al. (2003). Whole-mount staining of ovules was also carried out as previously published (Schneitz et al. 1995). Ovules at stage 3 were fixed for 2 h and stained with Mayer's haemalaun. For sections of immature seeds, the seeds were fixed for 16 h in fixation buffer (3.7% formaldehyde; 5% acetic acid; 1×PBS), dehydrated in an ethanol series and embedded in Technovit (Heraeus, Kulzer, Germany). Sections (4μm) were stained for several minutes with toluidine blue. Whole-mount vanillin staining was performed as described in Debeaujon et al. (2003).

Yeast-2/3-hybrid analysis

For yeast-two-hybrid analyses the GAL4-based Matchmaker System III (Clontech, San Jose, CA, USA) was used. The full-length *ABS* ORF was subcloned into the bait vector pGBKT7 using *Eco*RI and *Sal*I restriction sites. The construct was then tested for autoactivation in yeast strains AH109 and Y187. For the interaction screen, the *ABS*::pGBKT7 construct was transformed into the yeast strain Y187. A mixed *Arabidopsis* cDNA library of randomly primed and polyA-tailed cDNAs from total plant tissues of *A. thaliana* was cloned into pGADT7-REC and transformed into the yeast strain AH109. The screen was carried out by mating the two strains according to the manufacturer's instructions. About 52×10^6 diploids were obtained by mating. To screen for interacting proteins, diploids were spread on -Leu/-Trp/-His and -Leu/-Trp/-His/-Ade plates (both types supplemented with 3 mM 3-AT). Clones that grew on these selective plates within 3 days were picked and streaked on -Leu/-Trp/-His/-Ade plates containing 5 mM 3-AT and 10 mM 3-AT. A non-lethal β-galactosidase assay was performed (Duttweiler 1996) and clones that developed a strong blue colour after 1 h were analysed further by PCR (Ling et al. 1995) using vector primers to amplify the insert; the amplified product was then sequenced. Full-length clones and 3′-terminal deletion derivatives of the identified genes for putative interaction partners were cloned into pGBKT7 and pGADT7 and transformed into AH109 to confirm the interactions. All were routinely tested for autoactivation.

Domain deletion constructs of ABS were analysed for interaction with SEP3-IK. Interaction could only be tested in one direction because some of the binding domain fusions showed autoactivation. Coding sequence fragments with artificial *Eco*RI and *Bam*HI restriction sites and stop codons (where necessary) were obtained by PCR using modified primers; the additional sequences, plus 4–5 arbitrary bases which are required later for binding of the restriction enzyme, were attached to the 5′ ends of gene-specific primers. The following constructs were produced in pGADT7: ABS-MIK1 (encoding amino acids 1–114 of the protein sequence), ABS-K1-K3 (amino acids 87–176), ABS-K1-C (amino acids 87–stop), ABS-K2-K3 (amino acids 113–176) and ABS-K2-C (amino acids 113–stop). The constructs harboured either the natural stop codon or (in 3′-deleted versions) an artificial in-frame stop codon. The BD and AD constructs were cotransformed into AH109 and tested for interaction in a dilution series on SD-Leu/-Trp/-His plates containing 3 mM 3-AT. Constructs containing deletion derivatives of the *ABS* coding sequence in pGBKT7 were tested for autoactivation on SD-Trp-His containing 3 mM 3-AT.

Ternary complex formation was tested using different combinations of *ABS*, *SEP3* and *SHP1*, *SHP2*, *STK* or *AG* coding sequences transformed into pGBKT7, pGADT7 (Clontech) and pTFT1 (Egea-Cortines et al. 1999). The pGBKT7 and pGADT7 constructs were co-transformed into AH109, pTFT1 constructs were transformed into Y187. After small-scale mating following the protocol of Causier and Davies (2002), the

diploids were tested for interaction on -Leu/-Trp/-Ade/-His plates supplemented with 3 mM 3-AT, both at room temperature (22°C) and at 28°C for 6 days. In addition, a LacZ test was performed (Duttweiler 1996). Dimerization under similar conditions was tested using the empty pTFT1 vector and the same combinations of BD and AD constructs. The *ABSΔC*::pGBKT7 construct encodes amino acids 1–171 of the ABS protein.

Gel retardation assays

Gel retardation assays were performed essentially as described by Winter et al. (2002b). The *ABS* and *ABS*-MIK coding regions were cloned into the pSPUTK vector using *Bgl*II sites which were introduced by PCR. The full-length *SEP3* coding sequence was cloned using *Nco*I and *Eco*RI restriction sites. We used a CArG-Box sequence from the second intron of *AGAMOUS* (Gomez-Mena et al. 2005) as the probe (5′-GAAATTTAATTATATTCCAAA TAAGGAAAGTATGGAACGT T-3′). We also tested a mutant version of this sequence (mutCArG; 5′-GAAAT TTAATTATATTCCAAGTAAGGAAAGTATGGAA CGTT-3′). The probes were biotinylated at their 5′ ends, and 20 fmol of probe was used per lane. For competition experiments, unlabelled CArG-box-containing DNA, or control DNA without a CArG-box (sequence: 5′-CCTATCTGGGTAGCATATGCTATCC-3′) was added to the binding reaction in 100- or 50-fold molar excess as indicated below. After electrophoresis, the gels were blotted to positively charged nylon membranes (Hybond N+, Amersham) and signal detection was done using the chemiluminescent nucleic acid detection module (Pierce, Rockford, IL, USA).

Subcellular localization of ABS

The *ABS*::*CFP*/*YFP* constructs were cloned into pGD120 (Immink et al. 2002) using restriction sites that were introduced by PCR on both sites of the coding sequences for *ABS* and the fluorescent reporter proteins. For the fluorophores, *Xba*I and *Xho*I restriction sites were used to construct *CFP*::pGD120 and *YFP*::pGD120. The *ABS* ORF was introduced 5′ to and in frame with the FP coding sequences using *Sal*I and *Bam*HI sites. Transfection of *A. thaliana* protoplasts was performed as described for *Nicotiana tabacum* by Reidt et al. (2000). An embryogenic suspension culture produced from the roots of *A. thaliana* Col-24 was used (kindly provided by A. Tewes, IPK, Gatersleben). Localization of ABS::CFP/YFP fusion proteins in protoplasts was carried out by confocal scanning laser microscopy (CSLM) on a CSLM 510 Meta (Zeiss, Jena). Excitation was provided by the 458 and 514 nm argon laser. Three dichroic beam splitters were used to separate excitation from emission and to divide the fluorescence emission into the CFP, YFP and chlorophyll channels. Images were analysed and adapted with Zeiss LSM510 software and the program IrfanView Version 3.80 (http://www.irfanview.de).

Phylogenetic analysis

Protein-based cDNA-alignments were produced using the RevTrans tool http://www.cbs.dtu.dk/services/RevTrans/. Sites with gaps and the complete C-terminal coding sequence were deleted from the alignment, leaving an alignment of 384 sites. Different outgroups were tested. Neighbour-Joining analyses were performed using the Mega2 program (Kumar et al. 2001). The gamma shape parameter was calculated using the computer program Gamma with a Poisson Correction based tree as input. Bayesian analyses were done using MrBayes (Huelsenbeck and Ronquist 2001) with standard settings, gamma distributed rates and 1×10^6 generations, sampling every 50th generation.

The plantGDB (http://www.plantgdb.org/) was screened for B_{sister} genes in various species of flowering plants. Accession numbers of the ESTs are as follows: *LBS* (*LYCOPERSICON BSISTER*; *Solanum lycopersicum*): AI486443, AI899235 (assembled into contig LEtuc02-10-21.1808); *HBS2* (*HORDEUM BSISTER2*; *Hordeum vulgare*): BQ753907, CK122890, BM099355 (contig HVtuc02-11-10.10527); *HBS1* (*HORDEUM BSISTER1; H.vulgare*): CK125001, BQ764751, BM098919, (contig HVtuc02-11-10.11548), BU979626, BU981513, CK122554, BU974717; *ZMM32 (Zea mays MADS 32)*: AI964627.1, CO525542.1, CO534754.1.

Results

Novel loss-of-function alleles confirm that ABS plays a role in endothelium development

Arabidopsis abs mutants show structural defects in endothelium formation—the cell layer of the ovule in which PAs are specifically synthesized—and are affected in PA accumulation (Nesi et al. 2002). To investigate whether the mutant alleles of *ABS* reported previously display the null mutant phenotype, novel knock-out alleles were identified by reverse genetics. Screening of the ZIGIA population of transposon insertion lines identified two lines, 7K66 and 7AAL63, which were analysed further. Line 7AAL63 harbours a transposon insertion in the third intron of the *ABS* locus (Fig.1). The transposon shows a large internal deletion and has a total length of only about 2.6 kb (data not shown). Line 7K66 carries an insertion in the 3′UTR, several bases downstream of the stop codon (Fig.1). In accordance with the nomenclature used by Nesi et al. (2002), we have termed the novel mutant alleles *tt16-4* (line 7K66) and *tt16-5* (7AAL63). The seeds of plants from both lines showed an unstable transparent testa phenotype, displaying a range of colours from a wild type like brown to yellowish with a dark brown micropylar and chalazal end

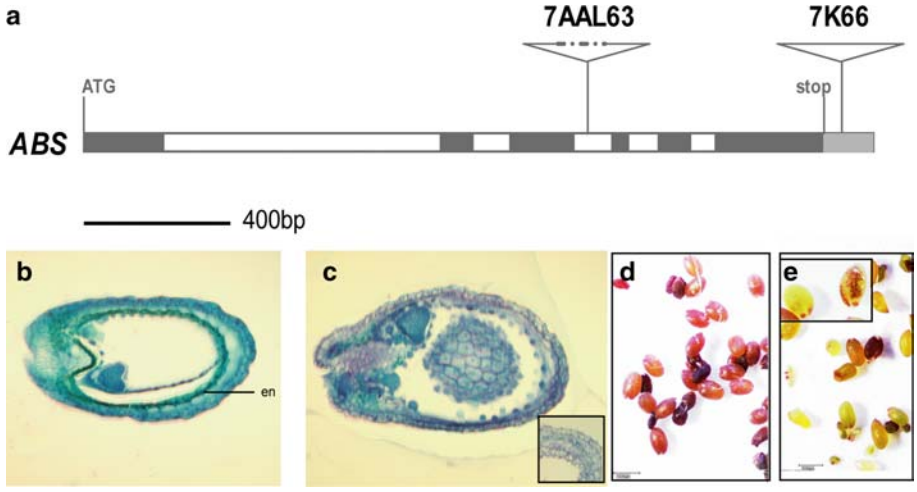

Fig. 1 Analysis of *ABS En1* insertion lines. **a** Schematic representation of the *ABS* locus including the transcribed sequence from the translational start codon (*ATG*) into the untranslated sequence downstream of the translational stop codon (*Stop*). The exon–intron structure is indicated, with exons shown in *dark grey*, the 3′UTR in *light grey* and the introns as *open boxes*. The sites of the transposon insertions in the two mutant lines are indicated by the *arrowheads*. **b** Cross-section through a toluidine-blue stained wild-type seed; the embryo is at heart stage. **c** Cross-section through a seed from a 7AAL63 (*tt16-5*) plant; *the inset* shows the integument structures of another seed at a higher magnification. **d**,**e** Vanillin staining of immature wild-type seeds (**d**) and seeds from the line 7AAL63 (e); the *inset* in **e** shows a close up. *en* endothelium

(Fig.1). For two representative plants of each line the accumulation of precursors of PAs was tested by vanillin staining (Fig.1). Irregular patterns of staining similar to those observed in mature seeds were obtained and residual 'background' production of PAs in line 7K66 was observed after prolonged staining. In addition, seed anatomy was analysed by toluidine staining of sections of immature seeds (Fig.1).

Sequencing of PCR-amplified alleles revealed multiple somatic excision events, indicating that the mosaic-like phenotype (Fig. 1e) might be due to the genetic instability of the insertion of the *En* transposable element at the *ABS* locus. Due to the formation of revertant sectors by somatic excision of the *En* element, a straightforward distinction between true heterozygotes and homozygotes was not possible.

Aside from its genetic instability, the mutant phenotype of the two novel insertion alleles *tt16-4* and *tt16-5* almost perfectly matches that of previously described putative null alleles (Nesi et al. 2002). These results suggest that the observed phenotype is very probably caused by the mutation in the *ABS* locus, although Southern analyses revealed the presence of approximately 8–10 copies of the *En*-transposon in both lines (data not shown). Moreover, the mutant phenotypes of the novel alleles strongly corroborate the view that the changes in seed colour and endothelial cell structure represent the null phenotype of *ABS*. We therefore chose not to investigate these lines further.

Analysis of 35S::ABS gain-of-function mutants

To gain further insight into the function of *ABS* the analysis of loss-of-function mutants was complemented by a detailed investigation of transgenic gain-of-function lines, in which the *ABS* coding region was expressed under the control of the CaMV 35S promoter. The expressivity and penetrance of the phenotypes in the T2 generation varied. A survey of the T2 generation of Basta-resistant T1 lines showed that, in this case, 21 of 44 lines showed a phenotype in the T2 generation (10 plants per T1 line were sown). The weaker phenotypes of 35S::*ABS* plants resembled those previously described by Nesi et al. (2002).

We also observed stronger phenotypes, which have not been described previously. These are characterized by a strong curling of the leaves, infertility, and floral homeotic changes (Fig. 2a–f). Plants with a strong phenotype were usually smaller than wild-type plants. In contrast to wild type, flowers were open during all developmental stages, starting from bud initiation. Moreover, the developmental timing of relative organ growth was disturbed leading to enhanced growth of carpels relative to other organs. Frequently some of the inflorescence meristems of the plants terminated in a compound structure consisting of carpeloid and stamenoid organs (Fig. 2a, c, e, f), and bracts having mosaic structures, made up of carpeloid or stamenoid elements and vegetative parts (Fig. 2d, g). The infertility may have been caused partly by defects in stamen elongation at the stage of anthesis and partly by a decrease in the production of mature pollen (Fig. 2e, f, and unpublished observations).

Flowers displaying strong phenotypes were further examined by scanning electron microscopy (Fig. 2i–n). Sepal cell structure was particularly strongly affected in these plants (Fig. 2j). The outer sepal surface of mature wild-type flowers consists of a mixture of long and short, irregularly shaped, epidermal cells (Fig. 2l), which become distinguishable from other cell types at stage 8 of flower development (Smyth et al. 1990). In contrast, the cell pattern of 35S::*ABS* sepals is regular and more like

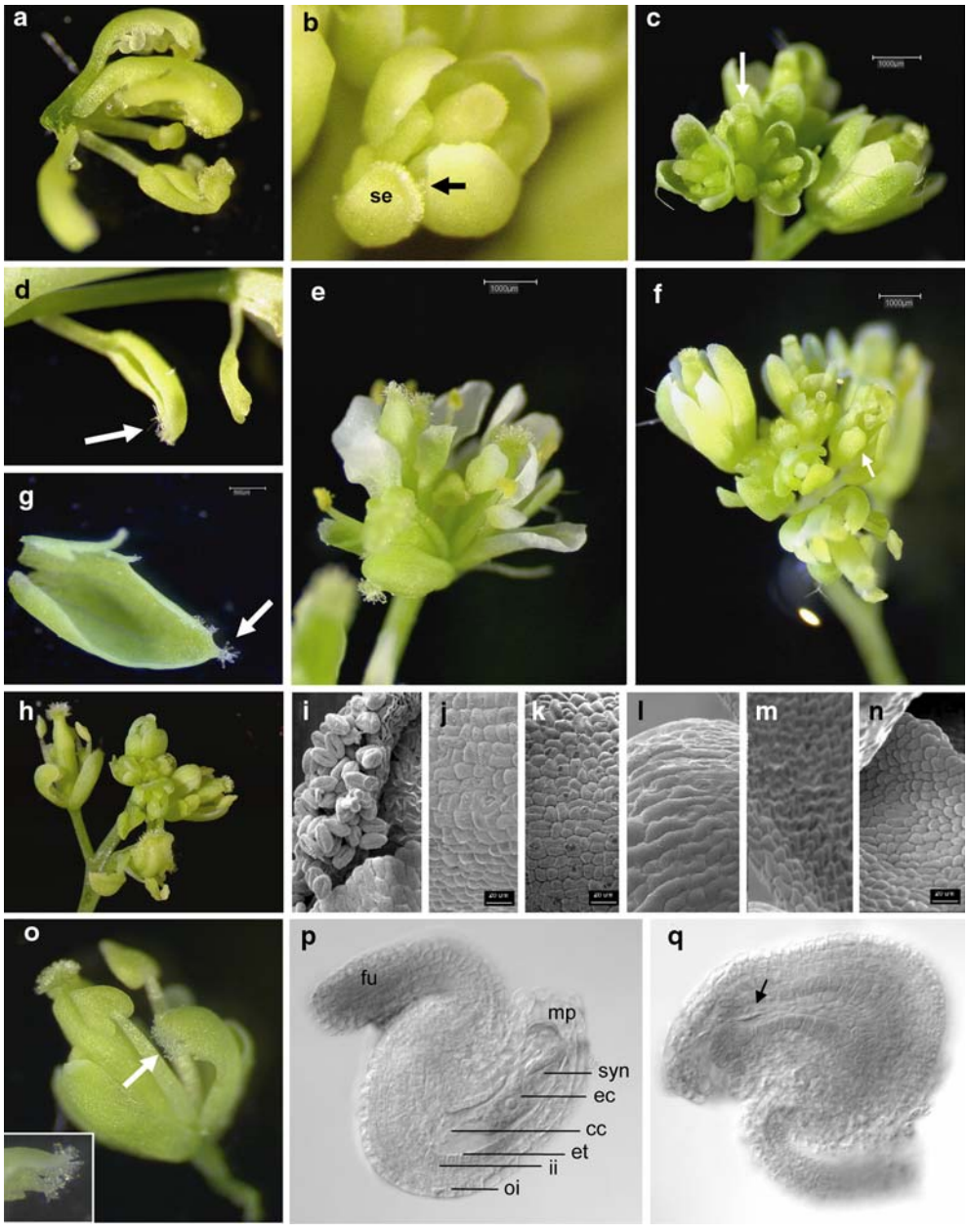

Fig. 2 Flower phenotypes of 35S::*ABS* transgenic plants. **a** Flower with homeotic transformations. **b** Flower with stigmatic tissue on the sepal margin. **c** Compound inflorescence. **d**, **g** Cauline leaves with stigmatic tissue at the margin (*arrows*). **e**,**f** Compound terminal inflorescences with mosaic-like homeotically transformed organs having carpeloid and stamenoid characteristics. **h** Compound terminal inflorescence of 35S::*ABS*-MIK plant. **i**–**n** SEM pictures of floral structures of *Arabidopsis* plants. **i** Pollen sacs with pollen. **j** Abaxial sepal surface. **k** Carpel surface. **l** Abaxial sepal surface of wild-type flower. **m** Adaxial petal surface of wild-type flower. **n** Adaxial petal surface of transgenic flower. **o** Flower of 35S::*ABS*-MIK plant with stigmatic tissue on first whorl sepal. **p** Wild-type ovule. **q** Sterile ovule from a 35S::*ABS* transgenic plant. *cc* central cell, *ec* egg cell, *et* endothelium, *fu* funiculus, *ii* inner integument, *mp* micropyle, *oi* outer integument, *p* petal, *se* sepal, *st* stamen, *syn* synergids

the carpel type (Fig. 2j, k). The carpeloid nature of sepal organs in 35S::*ABS* plants is further supported by the occasional presence of stigmatic tissue on the margins (Fig. 2b). Ovules were rarely formed on sepals (Fig. 2a). Stigmatic tissue was also sometimes observed on the margins of some bracts in late-appearing parts of the inflorescence.

Phenotypic analysis of 35S::*ABS*-MIK transgenic plants, which were transformed with constructs in which the region encoding the C-terminal domain of ABS was deleted, showed similar phenotypes (Fig. 2h, o). 35S::*ABS*-MIK plants displayed a curly leaf phenotype with early-opening flowers and, in some cases, partial homeotic transformations or terminal compound floral structures were observed (as in 35S::*ABS* plants).

To investigate the sterility defects further, we analysed ovule development by staining ovule whole mounts from several siliques of two sterile T2 plants of 35S::*ABS* plants. The nucellus was present in most ovules, but the embryo sac was often aborted at a very early stage of development (Fig. 2q). The incidence of this phenotype was higher (50–80%) in later appearing flowers than in those that opened early. The integument structure appeared irregular in some cases. Fertility was tested by applying wild-type pollen to siliques. Less than half of the tested ovules developed into seeds (i.e. had a functional embryo sac). In the embryos that developed, maturation was often delayed and reduced amounts of endosperm were formed (data not shown).

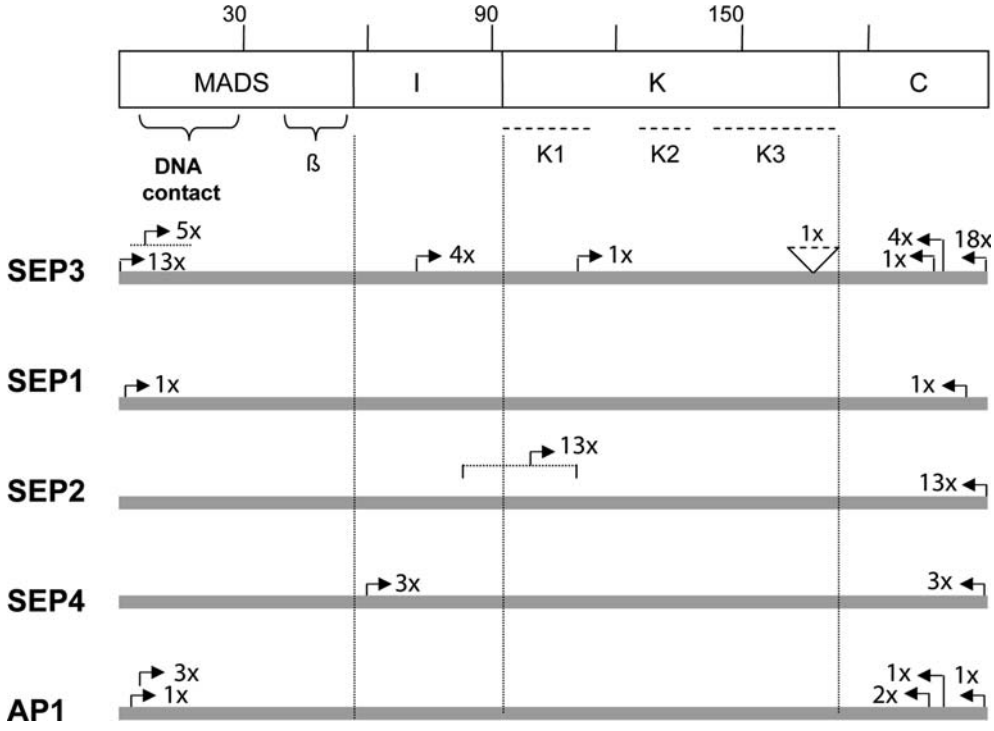

Fig. 3 Results of the yeast-two-hybrid screen using ABS as the bait. SEP3, SEP2, SEP1, SEP4 and AP1 were identified as interaction partners. The numbers of clones of each type recovered and their extents are indicated. The *triangle* marks a putative site of differential splicing in one clone of SEP3. The structure of MIKC-type proteins is shown schematically at the *top* (*numbers* correspond to amino acid positions). The MADS-domain includes the DNA-binding α-helix ('DNA contact) and a region (β), which forms β-sheets for protein–protein interactions. The potential coiled-coil forming units of the K-domain are also indicated (K1–K3)

Expression analysis using RT-PCR showed a strong *ABS* signal in the vegetative organs of transgenic 35S::*ABS* T2 plants, while no expression was detected in rosette leaves of wild-type *Arabidopsis* plants (data not shown). We then analysed the expression of *AG, STK, SHP1* and *SHP2* in the 35S::*ABS* plants. *SHP1*, *SHP2* and *STK* are MADS-box genes which have previously been shown to be required for ovule development, and produce comparable homeotic conversions of sepals into carpelloid organs when ectopically expressed (Favaro et al. 2003). However, overexpression of *SHP1* and *SHP2* can additionally induce homeotic transformation of petals to stamens similar to *AG* (Pinyopich et al. 2003). We also investigated the expression of *AGL63*, a closely related paralogue of *ABS* in *Arabidopsis* (see below). *AG, STK* and *AGL63* did not show any significant increase in expression in rosette leaves of 35S::*ABS* transgenic plants (data not shown). A slight increase in expression level was observed in some lines for *SHP1* and *SHP2*, but the effects of this weak expression in transgenic rosette leaves remain to be determined. It is likely that ectopic activation of these genes is more pronounced in the flower or inflorescence 'background', as has been observed in other transgenic plants that constitutively express *AG*-like genes and develop a phenotype that is similar to that of 35S::*ABS* plants (Favaro et al. 2003).

In summary, ectopic expression of *ABS* can affect the growth and identity of floral organs possibly by direct interaction with other floral homeotic genes (see below) or by ectopic activation of target genes.

Interaction partners of the ABS protein

A number of previous studies revealed that MADS-domain proteins form dimers or higher-order complexes to carry out their functions in flower and ovule development (Honma and Goto 2001; Theissen 2001; Favaro et al. 2003). The K-domain has been shown to function in protein interaction together with the MADS- and I-domains. The K-domain is characterized by three strings of heptad repeats [$(abcdefg)_n$] with hydrophobic amino acids predominating in the a and d positions. They probably constitute interaction surfaces involved in the formation of coiled coils (Fan et al. 1997; Yang et al. 2003). The heptad repeats are named K1, K2 and K3 (Fig. 3). Here we generally defined the K-domain as including a sequence that has traditionally been assigned to the C domain, but is predicted to be part of the K3 α-helix (Yang and Jack 2004).

In order to search for dimerization partners of ABS a yeast-two-hybrid assay was performed by screening an *Arabidopsis* cDNA library with the complete *ABS* coding region as the bait. Among the 55 clones obtained, 23 were identified as *SEP3*, four as *SEP2*, three as *SEP4* and one as *SEP1*; all these genes code for AGL2-like MADS-domain proteins (Fig. 3). Among the clones that gave weaker interaction signals, *APETALA1* (the gene for AP1, a SQUA-like protein) was found four times (Fig. 3).

As indicated in Fig. 3, the majority of *SEP3* clones that were identified (18/23) were full-length or were missing only 2–14 codons at their 5′ ends and had minor deletions of 3′-terminal sequences (all in the sequence

encoding the C-domain). Four of the expressed products started at amino acid (aa) position 71 in the I-domain, and one clone—which was among the strongest interactors—produced a protein consisting of domains K2 to C (starting at aa position 119 of the protein sequence) (Fig. 3). One of the clones had a deletion in the second half of K3, probably caused by a splicing defect that eliminated exon 6. The structures of all the identified SEP3, SEP1, SEP2 and AP1 segments produced by interacting clones are given in Fig. 3. The identified protein interactions were usually verified using full-length clones. For *SEP1* and *SEP3* in the bait vector, only clones that had C-terminal deletions were used in order to avoid autoactivation (Table 1). It was found that all tested interactions, except the one between SEP2 and ABS, worked in both directions (i.e., when cloned into bait or prey vector). The inability of the full-length SEP2 protein fused to the activation domain to interact with ABS is consistent with the fact that only N-terminally deleted versions were found in the screen (Fig. 3), suggesting a possible inhibitory effect of the MADS-domain on the interaction. This was only observed in one direction, however. Similar phenomena have been seen in other yeast-two-hybrid experiments with SEP2 (see, for example, Fornara et al. 2004). Furthermore, very weak homodimerization of ABS was observed in a test for homomeric interaction (Table 1).

For the protein–protein interaction most frequently observed in the yeast-two-hybrid screen—between ABS and SEP3—the approximate minimal interaction domain of ABS was determined. For that purpose several deletion constructs were cloned into the two-hybrid vectors (Fig. 4). Fusion proteins comprising the GAL4 binding domain linked to ABS sequences lacking the MADS-domain showed autoactivation in yeast, as revealed by growth on plates lacking histidine and supplemented with 3 mM 3-AT. Clear evidence for autoactivation was found with clones containing the C-terminal domain. This may be related to the presence of glutamine-rich stretches in the highly divergent C-terminal part of ABS. Autoactivation was abolished when the C-terminal domain was deleted, as shown for a construct comprising the complete K-domain (K1–K3). In light of these findings, the interaction of domain-deletion versions of ABS with SEP3 was only tested in one direction, using ABS sequences fused to the GAL4 activation domain. The distribution of clones identified in this screen suggested the K-domain as the minimal interaction domain of SEP3 required for interaction with ABS (Fig. 3). For that reason we used a SEP3 construct encoding the I- and K-domains fused to the GAL4 binding domain. In the interaction tests we identified the distal part (basically consisting of K2 and K3) of the K-domain to be the minimal domain of ABS necessary for interaction with SEP3 (Fig. 4).

Table 1 Confirmation of the interactions that were identified in the yeast-two-hybrid screen

Gene product[a]	ABS
SEP3*	+/+
SEP2	+/–
SEP1*	+/+
AP1	+/ND[b]
AGL3	+/+
ABS	(+)

[a]Interactions were generally tested in both directions (BD/AD). + indicates a positive interaction. Cases in which C-terminally deleted versions were used in the BD vector due to autoactivation of the full-length constructs are indicated by *asterisks*

[b]The interaction of ABS and AP1 was only tested in one direction (AP1 cloned into the AD vector) due to autoactivation. ABS is able to form relatively unstable homodimers

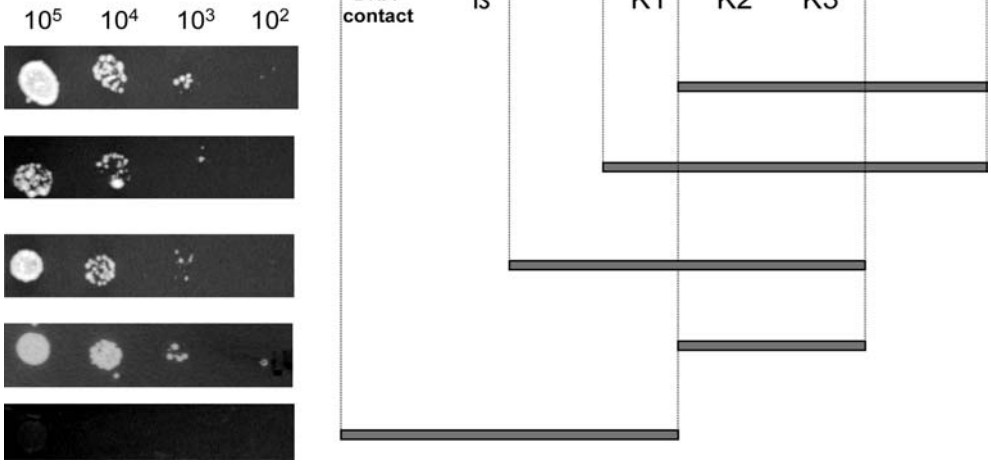

Fig. 4 Mapping of the minimal interaction domains of ABS and SEP3. A SEP3-IK construct was used as bait. Interaction was tested in a dilution series containing the indicated numbers of cells. Different C- and N-terminally deleted versions of ABS (depicted by the *grey bars*) were tested. A region comprising K2 and K3 appears to be sufficient for the interaction. The ABS protein sequence is depicted schematically at the *top* (*numbers* correspond to amino acid positions). The DNA contact and β regions are as defined in the legend to Fig.3. *K1*, *K2* and *K3* denote subdomains of the K-domain

Recently, Favaro et al. (2003) demonstrated the formation of higher-order complexes of MADS-domain proteins involved in ovule and carpel development. These protein complexes basically consist of combinations of SHP1, SHP2, STK ('D class') and AG ('C class') (all members of the AGAMOUS subfamily) and of the class E protein SEP3. As members of the AG clade have been shown to be expressed in ovules (see Discussion), we looked for evidence of a molecular interaction between ABS and members of the AG clade in ternary complexes containing SEP3, since no dimerization between ABS and AG occurs in yeast-two-hybrid experiments (data not shown). The full-length coding region of SEP3 was cloned into the ternary vector pTFT1. We screened at 28°C and 22°C, because previous studies have shown that higher-order interactions of *Arabidopsis* MIKC-type proteins are more stable at lower temperatures (Honma and Goto 2001). We identified a STK-SEP3-ABS interaction at both 28°C (data not shown) and 22°C (Fig. 5). At 22°C we also identified a putative complex consisting of SHP1, SEP3 and ABS, and—much weaker—evidence for SHP2-SEP3-ABS (Fig. 5). Furthermore, interaction of STK-SEP3-ABSΔC was detected at 22°C, but not at 28°C, indicating that the C-terminus of ABS is not essential for the formation of higher-order complexes at 22°C, but enhances the interaction or stability of the complex at higher temperatures (Fig. 5).

Fig. 5 **a**,**b** Formation of ternary complexes comprising ABS, SEP3 (ternary vector) and members of the AG-like subfamily (SHP1, SHP2 and STK). The screen was performed at 22°C on selective -His-Ade-Leu-Trp plates supplemented with 3 mM 3-AT in a dilution series (**a**). Panel **b** shows a negative control in which the AD construct was replaced by 'empty vector' in order to test for autoactivation of BD + ternary vector. Tests for direct interaction between ABS and each of the AG-like proteins individually (ternary vector construct replaced by empty vector) also gave negative results under our conditions (data not shown). *BD* bait vector pGBKT7 providing binding domain; *pTFT1* ternary vector; *AD* prey vector pGADT7 providing activation domain

Formation of DNA-binding heterodimers by ABS and SEP3

Previous analyses and structural data have shown that MADS-domain proteins bind to specific DNA sequences (CArG-boxes; consensus $CC[A/T]_6GG$) as dimers (reviewed in Kaufmann et al. 2005). However, not all protein complexes that have been identified in yeast-two-hybrid or co-immunoprecipitation experiments have been shown to be capable of DNA binding (see, for example, Riechmann et al. 1996). To learn more about the nature of the interactions between ABS and SEP proteins we tested whether the ABS-SEP3 dimer is able to bind specifically to CArG-box DNA. This experiment also served as an independent control of the results obtained in the yeast-two-hybrid system. First we analysed the DNA-binding capacity of ABS and SEP3 separately. Like most MIKC-type proteins analysed so far, both ABS and SEP3 could bind to the DNA probes as homodimers. However, ABS bound less strongly to the CArG-box than SEP3 (Fig. 6a). Binding of labelled probe by ABS or SEP3 could be abolished almost completely by adding a 100-fold excess of unlabelled CArG-box containing DNA, but not CArG-box-free DNA to the reaction, thus revealing the specificity of these proteins for the CArG-box. In contrast, the ABS-MIK protein, in which the C-terminus of the protein was deleted, was very seriously impaired in binding to DNA on its own (Fig. 6b), owing to defects in DNA-binding or dimerization. DNA-binding was not completely abolished, however (Fig. 6b). When an excess of SEP3 was expressed in the presence of ABS-MIK and CArG-box DNA, two retarded bands were detected: the upper band corresponded to the SEP3 homodimer and the lower to the SEP3-ABS-MIK heterodimer (Fig. 6c). Thus the SEP3-ABS heterodimer detected in yeast-two hybrid experiments is able to bind to DNA. The CArG-box used in our experiments, the sequence of which matches the

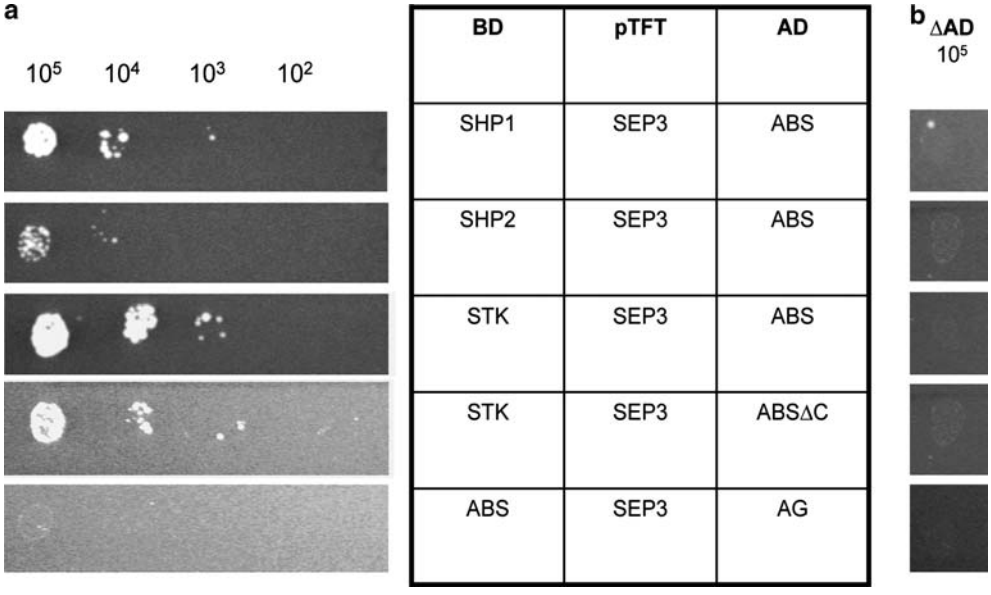

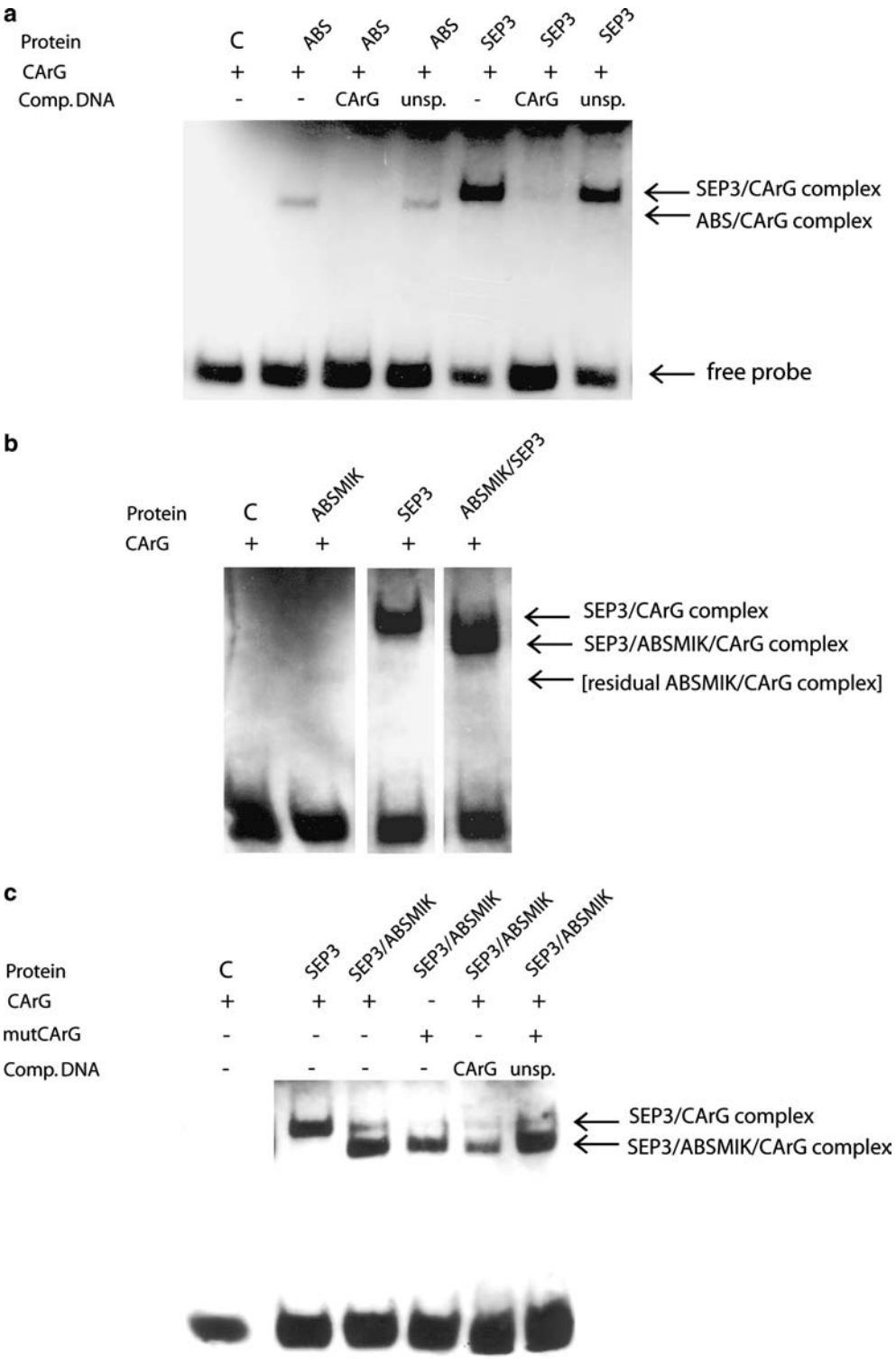

Fig. 6 Binding of ABS and SEP3 to CArG-box DNA sequences as revealed by gel retardation assays. **a** DNA-binding by full-length ABS and by the ABS-SEP3 complex, and effects of competition with unlabelled CArG-sequences and unspecific DNA, respectively. **b** Comparison of residual ABSMIK/CArG-complex with full-length SEP3/CArG- and SEP3/ABSMIK/CArG-complex. **c** Gel retardation and competition experiments showing formation of SEP3/CArG and SEP3/ABSMIK/CArG complexes. *CArG* CArG box sequence from the second intron of *AGAMOUS*, *mutCArG* the same sequence with a single nucleotide substitution (A− > G) in the core region of the CArG box, *C* negative control (reticulocyte extract); *Unsp.* unspecific (non-CArG), unlabelled competitor DNA

AG and AGL2 DNA recognition consensus sequences (Huang et al. 1996) almost perfectly, appeared to bind more strongly to the heterodimer than to the ABS homodimer.

Binding to the mutCArG-box which has a single A− > G substitution in the A/T core of the CArG sequence, was weaker but still detectable (Fig. 6c). That MADS-domain proteins can bind to CArG-boxes whose sequences deviate slightly from the consensus has been shown previously (Gomez-Mena et al. 2005). Addition of unlabelled CArG-box DNA significantly reduced the amount of labelled DNA that was shifted, while the addition of unlabelled CArG-box free DNA did not lead to a reduction in the level of shifted probe (Fig. 6c, last two lanes), demonstrating that the SEP3/ABSMIK heterodimer binds specifically to the CArG-box.

Subcellular localization of ABS

MIKC-type MADS-domain proteins are assumed to function in transcriptional regulation in the nucleus. We therefore tested whether ABS is indeed localized in the nucleus. Fusion proteins comprising ABS linked to the Yellow Fluorescent Protein (YFP) or the Cyan Fluorescent Protein (CFP) were expressed in *Arabidopsis* protoplasts under the control of the 35S promoter of the Cauliflower Mosaic Virus (CaMV). Investigation of the intracellular localization of the ABS::YFP and ABS::CFP proteins by confocal laser scanning microscopy (CLSM) revealed that both types of fusion proteins are located almost exclusively in the nucleus, while expression of CFP or YFP alone led only to diffuse fluorescence in the cell (Fig. 7). SEP3::CFP, STK::CFP, AP1::CFP, SEP1::YFP and AGL3::YFP fusion proteins were also clearly localized in the nucleus (data not shown). These data demonstrate that all these proteins can enter the nucleus alone or together with factors that are present in the protoplasts used.

Phylogenetic analysis of B_{sister} genes

In order to gain more insight into the evolutionary conservation of B_{sister} genes, phylogenetic and molecular evolutionary analysis were performed. An initial database screen for B_{sister} genes from other taxa was followed by phylogeny reconstructions. These analyses revealed the presence of two paralogous gene clades in the grass family (Poaceae) called the *ZMM17* clade sensu stricto and the *OsMADS31* clade. Representatives of both clades were found in rice (*Oryza sativa*), barley (*Hordeum vulgare*) and maize (*Zea mays*) (Fig. 8). In rice, a third paralogue is present, which seems to be more closely related to the *ZMM17* clade than to the others (Fig. 8). Furthermore, *AGL63* from *Arabidopsis* was identified as the most closely related paralogue of *ABS* in the *Arabidopsis* genome, in agreement with earlier indications (Parenicova et al. 2003). *AGL63* is an unusual gene, however, because it is characterized by a much faster rate of sequence evolution than *ABS* (as indicated by the longer branch length in the tree shown in Fig. 8) and by some deletions in the coding sequence. In their large-scale analysis of all *Arabidopsis* MADS-box genes, Parenicova et al. (2003) have shown that *AGL63* is expressed in inflorescences and siliques and also in roots. We confirmed the expression in flowers, which was very weak, and could detect no expression in vegetative leaves (data not shown).

Discussion

Analysis of new loss-of-function alleles of *ABS*

Two novel mutant alleles of the *ABS* gene, termed *tt16-4* and *tt16-5*, were identified in a screen of *En* insertion lines of *Arabidopsis*. Apart from their genetic instability due to frequent somatic reversions, the phenotypes of the two novel insertions match those of previously described putative null alleles *tt16-1*, *tt16-2* and *tt16-3* (Nesi et al. 2002). This corroborates the view that the observed changes in seed colour and endothelial cell structure represent the complete loss-of-function *abs*

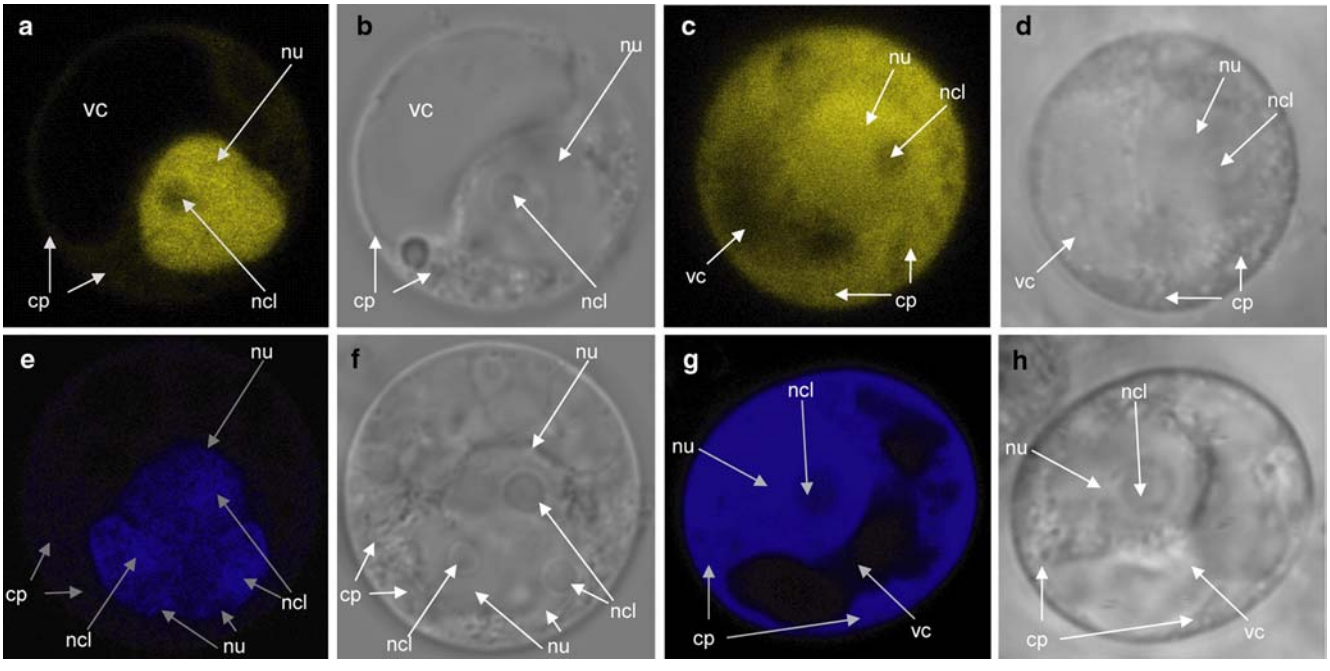

Fig. 7 ABS is localized in the nucleus in *Arabidopsis* protoplasts. **a**, **e** Nuclear localization of ABS::YFP and ABS::CFP, respectively. **c**, **g** Intracellular distribution of free YFP and CFP. The corresponding light micrographs are shown in panels **b**, **d**, **f** and **h**, respectively. *cp* cytoplasm, *ncl* nucleolus, *nu* nucleus, *vc* vacuole

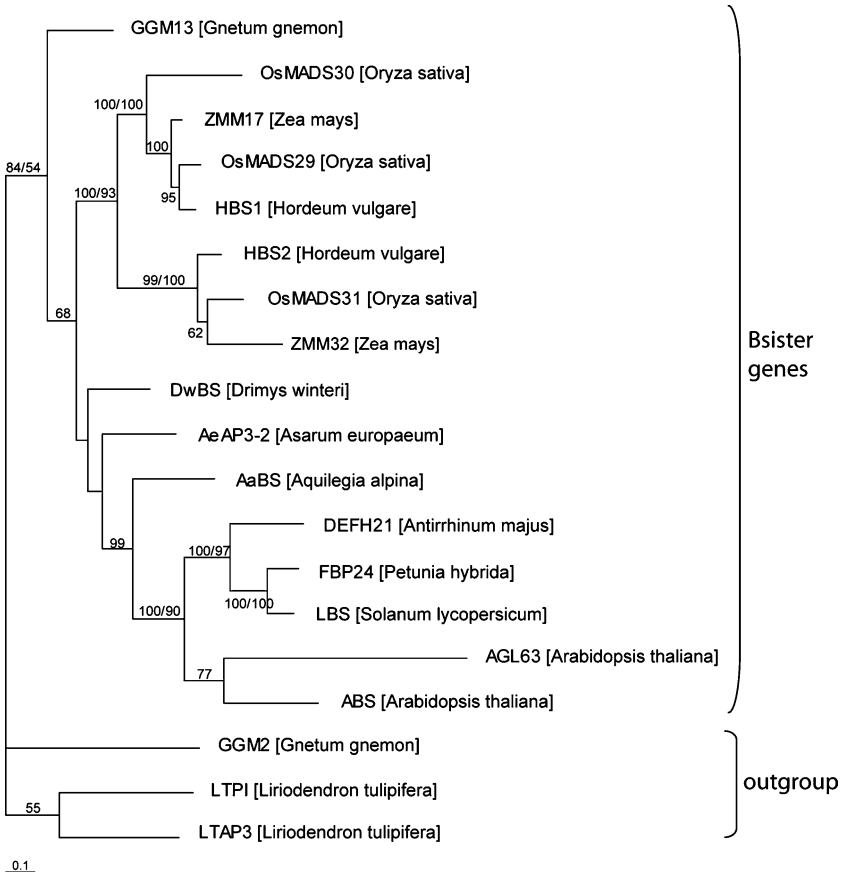

Fig. 8 Phylogenetic tree of B_{sister} genes. The tree was constructed using Bayesian methods and is based on a protein sequence alignment derived from cDNA sequences (381 sites). Bayesian "clade credibility values"/Bootstrap values (NJ K2P) are given next to the branches. The tree was rooted using B gene sequences as the outgroup (LTPI, LTAP3, GGM2)

phenotype. Thus, either the function of *ABS* is restricted to a role in endothelium development, or it is partially redundant to that of another gene, so that only the non-redundant part of the function is uncovered in *abs* null mutants. Distinguishing between these possibilities will require further studies. With *AGL63*, a closely related paralogue with a similar expression in reproductive organs has been identified that may share a function with *ABS*. Functional redundancy is quite a common phenomenon among *Arabidopsis* MIKC-type MADS-box genes. Well-characterized examples include *AP1*/*CAL*, *SHP1*/*SHP2* and *SEP1*/*SEP2*/*SEP3* (Ferrandiz et al. 2000; Liljegren et al. 2000; Pelaz et al. 2000). Ka/Ks analyses indicate that *AGL63* is under purifying selection and hence could be functional (Ka/Ks = 0.46). However, *agl63* loss-of-function mutants and *abs agl63* double mutants will be required before one can determine to what extent the functions of *ABS* and *AGL63* overlap.

ABS interacts with SEP proteins and the heterodimer forms higher-order complexes with AG-like proteins

MADS-domain proteins function as dimers and in higher-order complexes in flower and ovule development (Fan et al. 1997; Favaro et al. 2003; Honma and Goto 2001; Riechmann et al. 1996). Functional protein interactions in planta require spatial and temporal overlap in the expression profiles of interacting partners. In particular, higher-order complexes consisting of SHP1, SHP2, STK and SEP proteins have been proposed to determine ovule identity (Favaro et al. 2003). Studies on *SEP1*/*sep1 sep2 sep3* mutants also provided genetic evidence for a role of SEP proteins in ovule development.

We identified protein interactions between ABS and SEP1–3, AGL3 (recently renamed SEP4 by Ditta et al. 2004) and AP1. The interaction between ABS and SEP3, the one most often recovered in our two-hybrid screen, was confirmed by gel retardation experiments. ABS is also able to bind DNA as a homodimer, but strong binding requires the presence of the C-terminal domain. The requirement for this domain for the formation of DNA-binding homodimers has been reported for some B proteins previously (Tzeng et al. 2004; C. Weiser and G. Theissen, unpublished results). This provides an interesting corollary to the phylogenetic relationship between B and B_{sister} proteins, which have similar C-terminal motifs (Becker et al. 2002). The lower affinity of the ABS homodimer for the CArG sequence used in our experiments makes it possible that the homodimer has a generally lower capacity to form DNA-binding dimers relative to the heterodimer containing SEP3. Furthermore, the optimal DNA consensus sequence bound by the homodimer may differ from the sequence that was

provided here. Further experiments will be required to probe these aspects of ABS function.

We also found evidence for the formation of higher-order complexes containing ABS, SEP3 and the AG-like proteins STK, SHP1 and SHP2. Flanagan and Ma (1994) have described the expression of *SEP1* in ovules and developing seeds. *SEP1* is uniformly expressed in ovule and seed coat, as well as in the funiculus, also at later stages after fertilization, but expression levels fall as the seed matures. *SEP3* is also expressed in all tissues of ovules and developing seeds; its expression ceases during embryo development (Mandel and Yanofsky 1998). RT-PCR experiments show that *ABS* is expressed in floral buds, flowers and siliques (Nesi et al. 2002; confirmed by own, unpublished data). Furthermore, the *abs* loss-of-function phenotype implies a function in the development of the inner integument and the endothelium which begins before and continues after fertilization. Thus the expression domains of *ABS* and *SEP* genes may well overlap. For *SHP1*, detailed expression studies have shown that it is expressed in the developing and mature ovule, particularly in the endothelium (Flanagan et al. 1996). *STK* is expressed in all parts of ovules before and after fertilization; however, expression is strongest in the chalazal region and the funiculus (Rounsley et al. 1995). There is thus a clear overlap in the spatiotemporal domain of the *ABS* function and transcription of the genes for its interaction partners detected in yeast-2/3-hybrid analyses. This is compatible with an in planta function for the identified complexes. In situ hybridization has shown the B_{sister} gene of *Antirrhinum* to be expressed in the endothelium, and its homologue in the gymnosperm *Gnetum* is transcribed in similar tissues (Becker et al. 2002), indicating that the expression profile of B_{sister} genes has been conserved for at least 300 million years. Preliminary data suggest that *ABS* mRNA in *Arabidopsis* accumulates in the endothelium (Kaufmann 2001), but at much lower levels (near the limits of detection by *in situ* hybridization) than in *Antirrhinum*, so that the data obtained in *Arabidopsis* so far are not very reliable.

Our results suggest that SEP proteins not only form higher-order complexes with AG-like proteins, but that ABS also is part of these complexes. We have identified a specific interaction of ABS with STK, SHP1 and (much weaker) SHP2, but not with AG, in a higher-order complex. This complex might act in the specification of the inner integument layer of ovules.

The minimal interaction domains of ABS and SEP3 were mapped by deletion studies and the results indicate K2-K3 as the minimal interaction domain in yeast-two-hybrid studies. This is quite similar to the results obtained for the PI-SEP1 interaction (Yang et al. 2003). The K-domain, which is presumed to form coiled-coil structures, has been shown to be important for the interaction of MADS-domain proteins (Fan et al. 1997; Yang et al. 2003). Its role in higher-order complexes is not well understood, although our data from the yeast-two-hybrid screen suggest that the K-domain is important for the interactions that lead to higher-order complexes, because an ABS protein lacking the C-terminal domain was still able to form ternary complexes with SEP3/STK. However, these were comparatively less stable: the interaction was only observed at room temperature (22°C), suggesting that the C-terminal domain has a stabilizing effect on the interaction at higher (more stringent) temperatures.

Previous results indicated strongly that MIKC-type proteins are actively transported into the nucleus (rather than entering by simple diffusion) as dimers, despite the relatively small size of the protein monomers (~29 kDa) (see, for example, Immink et al. 2002). The nuclear localization of ABS demonstrated here (Fig. 7) is comparable to previous results for other MIKC-type proteins (Immink et al. 2002). Since ABS can homodimerize (Fig. 6a, and data not shown), it is not surprising that nuclear localization is observed when ABS alone is expressed in the protoplasts. Furthermore, it appears likely that in plant cells in which ABS and its potential interaction partners are co-expressed, these proteins are co-localized in the nucleus, and that those proteins that interact in two-hybrid or three-hybrid experiments in yeast indeed form active transcription factor complexes in planta.

Effects of ectopic expression of *ABS* in wild-type *Arabidopsis* plants

Constitutive expression of the ovule-specific MADS-box gene *ABS* leads to a number of defects in flower development, including early opening of flowers, partial homeotic conversion of sepals to carpeloid organs and, occasionally, the formation of compound floral structures consisting of stamenoid and carpeloid organs at the inflorescence tips (Fig. 2a, b, c, e, f, j). The floral defects that we observed might have been a result of functional interference with proteins that ABS normally encounters only in its normal expression domain (or not at all), or of ectopic activation of target genes of *ABS* that are usually induced only during ovule development. The second alternative appears unlikely, as 35S::*ABS*-MIK plants show similar phenotypes. In other cases, such as AGAMOUS, overexpression of MIKC-type proteins that were truncated in the C-terminal region resulted in dominant negative effects (Mizukami et al. 1996). The same can be assumed here also for ABS and, due to the similarity between the phenotypes of ABS-MIKC and ABS-MIK overexpressors, we consider it likely that the effects of full-length ABS are also brought about by a dominant negative effect.

Given the finding that ABS can interact with SEP proteins (and to a lesser extent with AP1), and form higher-order complexes with SEP and AG-like proteins, we suggest a model that explains the phenotypes largely in terms of dosage- and affinity-dependent titration of protein complexes involved in specifying floral organ identity. This could explain the majority of the defects observed in floral organ maturation and male fertility. In

the 35S::*ABS* plants, *ABS* is not only ectopically expressed throughout the plant, but its expression is also significantly up-regulated due to the use of the strong constitutive promoter. *ABS* could for instance prevent the *SEP* dependent up-regulation of the concentrations of floral homeotic proteins, by squelching SEP proteins.

Some homeotic functions may be more sensitive to relative protein concentrations in the cell than others. ABS is, in principle, able to remove two components of the protein complexes determining sepal and petal identity because it can interact with both AP1 and SEP proteins—and indeed some *ap1* mutant alleles (e.g. *ap1-3* and *ap1-10*) are associated with partial homeotic conversion of sepals to carpelloid organs (Bowman et al. 1993). For all MIKC-type proteins, it remains to be seen how (or whether) interaction strength in yeast-two-hybrid assays correlates with interaction strength in planta. In general, however, these phenotypes provide circumstantial evidence for the idea that the protein interactions that were found in the yeast experiments also occur in planta.

The homeotic transformation of first-whorl organs and the composite reproductive structures that sometimes appear at inflorescence tips may result from ABS-containing protein complexes that are functional only in the up-regulation of class C or D genes in floral organs or only a few of the downstream-targets of floral homeotic genes. Stamenoid and carpelloid organs could be produced by a partial replacement of B (or C) class proteins in complexes by ABS (or ABS-MIK) given the phylogenetic relationship and sequence similarity between B and B_{sister} proteins. However, this may only refer to targets that are bound by the ABS-MIK/SEP3 heterodimer (Fig. 6c), since the ABS-MIK homodimer may have lost its DNA-binding capacity almost completely (Fig. 6b). SEP3 is known to provide a strong activation domain that could in this case compensate for the missing C-terminal domain of ABS.

The compound floral structures that are produced in 35S::*ABS* and 35S::*ABS*-MIK plants are reminiscent of *tfl1*-like phenotypes, even though these structures usually arise much later in inflorescence development in 35S::*ABS* and 35S::*ABS*-MIK plants. *tfl1*-like phenotypes are associated with ectopic expression of floral meristem identity genes (*LFY*, *AP1*, *CAL*) in the inflorescence meristem. However, our Y2H screens using ABS as a bait provide no evidence for direct interactions between TFL and ABS, although this of course does not rigorously exclude such interactions in planta.

On the other hand, the finding that even 35S::*ABS* plants with strong phenotypes do not show ectopic formation of complete organs suggests either that *ABS* is not an organ identity gene or that its activity requires additional factors that are missing outside of its normal expression domain. We prefer the first hypothesis. Previous analyses have shown that *ABS* is involved in anthocyanin biosynthesis in the seed coat (Nesi et al. 2002; Debeaujon et al. 2003), which is confirmed by our data. The data also suggest a role of *ABS* in endothelium development. Both of these functions are obviously subordinate to organ identity, as they do not constitute organ identity itself. Interestingly, 35S::*ABS* plants with a strong phenotype sometimes show irregularities in the structure of the inner integument (not shown). In addition, embryo sac development is sometimes defective in these plants, and this is, at least in part, responsible for the female sterility. Embryos that develop after pollination with wild-type pollen show delayed growth, which is related to the small amounts of endosperm formed. These results may indicate that the effects of ectopic expression of *ABS* on overall plant development cause stress that leads to ovule abortion (Sun et al. 2004). Alternatively, proper timing of *ABS* expression at a specific level may be essential in ovule development. As sterility was observed in only a fraction of the plants overexpressing *ABS*, and impaired fertility was also noted in plants overexpressing *ABS*-MIK, the possibility can not be excluded that the phenotype is due to co-suppression phenomena that inhibit the function of closely related genes like *AGL63*.

Phylogeny of *GGM13*-like genes: gene duplications in monocots and *Arabidopsis*

The gene duplication which led to B and B_{sister} genes is phylogenetically ancient. It predates the origin of extant seed plants and may be related to the morphological evolution of seed-plant reproductive structures (Becker et al. 2002). B_{sister} genes show a conserved expression pattern in female reproductive organs, and may be 'marker genes' for the development of (inner) integument structures, which are the phylogenetically 'oldest' structures surrounding the female gametophyte of seed plants. Integuments are key innovations of seed plants that are related to the seed-plant specific form of heterospory, which is characterized by the retention of the female gametophyte on the mother plant. Our phylogenetic analysis has revealed the existence of a very divergent paralogue of *ABS* in *Arabidopsis*, *AGL63*.

We also identified a gene duplication in the B_{sister} gene clade leading to two paralogous subclades in the grass lineage of monocots. Loss-of-function mutations outside *Arabidopsis* should give us deeper insights into the evolutionary dynamics of B_{sister} gene function and its contribution to the evolution of female reproductive structures in seed plants.

Acknowledgements We thank Simona Masiero (MPIZ, Cologne) for valuable advice on the yeast-*n*-hybrid studies, Hans Sommer (MPIZ, Cologne) and Simona Masiero for providing the yeast-two-hybrid library and pTFT1 constructs, Ulrike Hartmann (MPIZ, Cologne) for providing yeast-two-hybrid plasmids encoding SEP proteins, and Richard Immink (PRI, Wageningen, Netherlands) for providing plasmid pGD120. We are also indebted to Pia Nutt for producing the 35S::*ABS*-MIK transgenic plants and for general practical support, and to Rainer Melzer for useful discussions and general support. Many thanks to Britta Grosardt (MPIZ, Cologne) for technical assistance, and to the members of the ZIGIA group for the filter screen of the *En1* population. We are grateful to Kay Schneitz (TU, Munich) for advice on the microscopic study of

ovule structure, and to Annegret Tewes, Michael Melzer, Bernhard Claus (IPK, Gatersleben) and Annette Becker for help with the nuclear localization studies. Thanks to members of the An lab (POSTECH, Korea) for sharing sequence information.

References

Becker A, Theissen G (2003) The major clades of MADS-box genes and their role in the development and evolution of flowering plants. Mol Phylogenet Evol 29:464–489

Becker A, Kaufmann K, Freialdenhoven A, Vincent C, Li MA, Saedler H, Theissen G (2002) A novel MADS-box gene subfamily with a sister-group relationship to class B floral homeotic genes. Mol Genet Genomics 266:942–950

Bowman JL, Alvarez J, Weigel D, Meyerowitz EM, Smyth DR (1993) Control of flower development in *Arabidopsis thaliana* by *APETALA1* and interacting genes. Development 119:721–743

Carlsbecker A, Sundstrom J, Tandre K, Englund M, Kvarnheden A, Johanson U, Engstrom P (2003) The *DAL10* gene from Norway spruce (*Picea abies*) belongs to a potentially gymnosperm-specific subclass of MADS-box genes and is specifically active in seed cones and pollen cones. Evol Dev 5:551–561

Causier B, Davies B (2002) Analysing protein–protein interactions with the yeast two-hybrid system. Plant Mol Biol 50:855–870

Debeaujon I, Nesi N, Perez P, Devic M, Grandjean O, Caboche M, Lepiniec L (2003) Proanthocyanidin-accumulating cells in *Arabidopsis* testa regulation of differentiation and role in seed development. Plant Cell 15:2514–2531

Ditta G, Pinyopich A, Robles P, Pelaz S, Yanofsky MF (2004) The *SEP4* gene of *Arabidopsis thaliana* functions in floral organ and meristem identity. Curr Biol 14:1935–1940

Duttweiler HM (1996) A highly sensitive and non-lethal beta-galactosidase plate assay for yeast. Trends Genet 12:340–341

Egea-Cortines M, Saedler H, Sommer H (1999) Ternary complex formation between the MADS-box proteins SQUAMOSA, DEFICIENS and GLOBOSA is involved in the control of floral architecture in *Antirrhinum majus*. EMBO J 18:5370–5379

Fan HY, Hu Y, Tudor M, Ma H (1997) Specific interactions between the K domains of AG and AGLs, members of the MADS domain family of DNA binding proteins. Plant J 12:999–1010

Favaro R, Pinyopich A, Battaglia R, Kooiker M, Borghi L, Ditta G, Yanofsky MF, Kater MM, Colombo L (2003) MADS-box protein complexes control carpel and ovule development in Arabidopsis. Plant Cell 15:2603–2611

Ferrandiz C, Gu Q, Martienssen R, Yanofsky MF (2000) Redundant regulation of meristem identity and plant architecture by FRUITFULL, APETALA1 and CAULIFLOWER. Development 127:725–734

Flanagan CA, Ma H (1994) Spatially and temporally regulated expression of the MADS-box gene *AGL2* in wild-type and mutant *Arabidopsis* flowers. Plant Mol Biol 26:581–595

Flanagan CA, Hu Y, Ma H (1996) Specific expression of the *AGL1* MADS-box gene suggests regulatory functions in *Arabidopsis gynoecium* and ovule development. Plant J 10:343–353

Fornara F, Parenicova L, Falasca G, Pelucchi N, Masiero S, Ciannamea S, Lopez-Dee Z, Altamura MM, Colombo L, Kater MM (2004) Functional characterization of *OsMADS18*, a member of the AP1/SQUA subfamily of MADS box genes. Plant Physiol 135:2207–2219

Gomez-Mena C, de Folter S, Costa MM, Angenent GC, Sablowski R (2005) Transcriptional program controlled by the floral homeotic gene *AGAMOUS* during early organogenesis. Development 132:429–438

Grossniklaus U, Schneitz K (1998) The molecular and genetic basis of ovule and megagametophyte development. Semin Cell Dev Biol 9:227–238

Honma T, Goto K (2001) Complexes of MADS-box proteins are sufficient to convert leaves into floral organs. Nature 409:525–529

Huang H, Tudor M, Su T, Zhang Y, Hu Y, Ma H (1996) DNA binding properties of two Arabidopsis MADS domain proteins: binding consensus and dimer formation. Plant Cell 8:81–94

Huelsenbeck JP, Ronquist F (2001) MRBAYES: bayesian inference of phylogenetic trees. Bioinformatics 17:754–755

Immink RG, Gadella TW Jr, Ferrario S, Busscher M, Angenent GC (2002) Analysis of MADS box protein–protein interactions in living plant cells. Proc Natl Acad Sci USA 99:2416–2421

Kaufmann K (2001) Molekulare Charakterisierung von Kandidatengenen für die Spezifizierung weiblicher Reproduktionsorgane in Angiospermen und Gymnospermen. Diploma Thesis, Friedrich Schiller University, Jena

Kaufmann K, Melzer R, Theissen G (2005) MIKC-type MADS-domain proteins: structural modularity, protein interactions and network evolution in land plants. Gene 347:183–198

Kumar S, Tamura K, Jakobsen IB, Nei M (2001) MEGA2: molecular evolutionary genetics analysis software. Bioinformatics 17:1244–1245

Liljegren SJ, Ditta GS, Eshed Y, Savidge B, Bowman JL, Yanofsky MF (2000) *SHATTERPROOF* MADS-box genes control seed dispersal in Arabidopsis. Nature 404:766–770

Ling M, Merante F, Robinson BH (1995) A rapid and reliable DNA preparation method for screening a large number of yeast clones by polymerase chain reaction. Nucleic Acids Res 23:4924–4925

Ma H, Yanofsky MF, Meyerowitz EM (1991) *AGL1–AGL6*, an *Arabidopsis* gene family with similarity to floral homeotic and transcription factor genes. Genes Dev 5:484–495

Mandel MA, Yanofsky MF (1998) The Arabidopsis *AGL9* MADS box gene is expressed in young flower primordia. Sex Plant Repr 11:22–28

Mizukami Y, Huang H, Tudor M, Hu Y, Ma H (1996) Functional domains of the floral regulator AGAMOUS: characterization of the DNA binding domain and analysis of dominant negative mutations. Plant Cell 8:831–845

Nesi N, Debeaujon I, Jond C, Stewart AJ, Jenkins GI, Caboche M, Lepiniec L (2002) The *TRANSPARENT TESTA16* locus encodes the ARABIDOPSIS BSISTER MADS domain protein and is required for proper development and pigmentation of the seed coat. Plant Cell 14:2463–2479

Parenicova L, de Folter S, Kieffer M, Horner DS, Favalli C, Busscher J, Cook HE, Ingram RM, Kater MM, Davies B, Angenent GC, Colombo L (2003) Molecular and phylogenetic analyses of the complete MADS-box transcription factor family in *Arabidopsis*: new openings to the MADS world. Plant Cell 15:1538–1551

Pelaz S, Ditta GS, Baumann E, Wisman E, Yanofsky MF (2000) B and C floral organ identity functions require *SEPALLATA* MADS-box genes. Nature 405:200–203

Pinyopich A, Ditta GS, Savidge B, Liljegren SJ, Baumann E, Wisman E, Yanofsky MF (2003) Assessing the redundancy of MADS-box genes during carpel and ovule development. Nature 424:85–88

Reidt W, Wohlfarth T, Ellerstrom M, Czihal A, Tewes A, Ezcurra I, Rask L, Bäumlein H (2000) Gene regulation during late embryogenesis: the RY motif of maturation-specific gene promoters is a direct target of the FUS3 gene product. Plant J 21:401–408

Riechmann JL, Krizek BA, Meyerowitz EM (1996) Dimerization specificity of Arabidopsis MADS domain homeotic proteins APETALA1, APETALA3, PISTILLATA, and AGAMOUS. Proc Natl Acad Sci USA 93:4793–4798

Rounsley SD, Ditta GS, Yanofsky MF (1995) Diverse roles for MADS box genes in Arabidopsis development. Plant Cell 7:1259–1269

Sagasser M, Lu GH, Hahlbrock K, Weisshaar B (2002) *A. thaliana* TRANSPARENT TESTA 1 is involved in seed coat development and defines the WIP subfamily of plant zinc finger proteins. Genes Dev 16:138–149

Schneitz K, Hülskamp M, Pruitt RE (1995) Wild-type ovule development in *Arabidopsis-t haliana*—a light-microscope study of cleared whole-mount tissue. Plant J 7:731–749

Smyth DR, Bowman JL, Meyerowitz EM (1990) Early flower development in Arabidopsis. Plant Cell 2:755–767

Steiner-Lange S, Gremse M, Kuckenberg M, Nissing E, Schachtele D, Spenrath N, Wolff M, Saedler H, Dekker K (2001) Efficient identification of Arabidopsis knock-out mutants using DNA-arrays of transposon flanking sequences. Plant Biol 3:391–397

Stellari GM, Jaramillo MA, Kramer EM (2004) Evolution of the *APETALA3* and *PISTILLATA* lineages of MADS-box-containing genes in the basal angiosperms. Mol Biol Evol 21:506–519

Sun K, Hunt K, Hauser BA (2004) Ovule abortion in Arabidopsis triggered by stress. Plant Physiol 135:2358–2667

Theissen G (2001) Development of floral organ identity: stories from the MADS house. Curr Opin Plant Biol 4:75–85

Töpfer R, Matzeit V, Gronenborn B, Schell J, Steinbiss HH (1987) A set of plant expression vectors for transcriptional and translational fusions. Nucleic Acids Res 15:5890–5890

Tzeng TY, Liu HC, Yang CH (2004) The C-terminal sequence of LMADS1 is essential for the formation of homodimers for B function proteins. J Biol Chem 279:10747–10755

Unte US, Sorensen AM, Pesaresi P, Gandikota M, Leister D, Saedler H, Huijser P (2003) *SPL8*, an SBP-Box gene that affects pollen sac development in Arabidopsis. Plant Cell 15:1009–1019

Winter KU, Saedler H, Theissen G (2002a) On the origin of class B floral homeotic genes: functional substitution and dominant inhibition in Arabidopsis by expression of an orthologue from the gymnosperm *Gnetum*. Plant J 31:457–475

Winter KU, Weiser C, Kaufmann K, Bohne A, Kirchner C, Kanno A, Saedler H, Theissen G (2002b) Evolution of class B floral homeotic proteins: obligate heterodimerization originated from homodimerization. Mol Biol Evol 19:587–596

Yang Y, Jack T (2004) Defining subdomains of the K domain important for protein–protein interactions of plant MADS proteins. Plant Mol Biol 55:45–59

Yang Y, Fanning L, Jack T (2003) The K domain mediates heterodimerization of the Arabidopsis floral organ identity proteins, APETALA3 and PISTILLATA. Plant J 33:47–59